2014 American Control Conference (ACC)
June 4-6, 2014. Portland, Oregon, USA

Completion of partially known turbulent flow statistics

Armin Zare, Mihailo R. Jovanović, and Tryphon T. Georgiou

Abstract— **Second-order statistics of turbulent flows can be obtained either experimentally or via high fidelity numerical simulations. The statistics are relevant in understanding fundamental flow physics and for the development of low-complexity models. For example, such models can be used for control design in order to suppress or promote turbulence. Due to experimental or numerical limitations it is often the case that only partial flow statistics are known. In other words, only certain correlations between a limited number of flow field components are available. Thus, it is of interest to complete the statistical signature of the flow field in a way that is consistent with the known dynamics. Our approach to this inverse problem relies on a model governed by stochastically forced linearized Navier-Stokes equations. In this, the statistics of forcing are unknown and sought to explain the given correlations. Identifying suitable stochastic forcing allows us to complete the correlation data of the velocity field. While the system dynamics impose a linear constraint on the admissible correlations, such an inverse problem admits many solutions for the forcing correlations. We use nuclear norm minimization to obtain correlation structures of low complexity. This complexity translates into dimensionality of spatio-temporal filters that can be used to generate the identified forcing statistics.**

Index Terms— **Convex optimization, flow control, low-rank approximation, stochastically forced Navier-Stokes equations, structured matrix completion problems, turbulence modeling.**

I. Introduction

Nonlinear dynamical models for turbulent fluid flow that are based on the Navier-Stokes (NS) equations typically have a large number of degrees of freedom which makes them unsuitable for control synthesis. Thus, for the purpose of control design, several techniques have been proposed for obtaining low-dimensional models that preserve the essential dynamics. In particular, linearization of the NS equations around mean-velocity, driven by white-in-time stochastic excitation has been shown to provide satisfactory models that qualitatively replicate structural features of wall-bounded shear flows [1]–[4]. However, it has also been recognized that white-in-time stochastic forcing is too restrictive to reproduce all statistical features of the fluctuating velocity field [5]. In the present work we study colored-in-time stochastic excitation of the linearized dynamics. Building on [6], we derive low-complexity dynamical models that can successfully account for all observed second-order statistics that may be available from experiments or numerical simulations.

Financial support from the University of Minnesota Initiative for Renewable Energy and the Environment under Early Career Award RC-0014-11 is gratefully acknowledged. The University of Minnesota Supercomputing Institute is acknowledged for providing computing resources.

Armin Zare, Mihailo R. Jovanović, and Tryphon T. Georgiou are with the Department of Electrical and Computer Engineering, University of Minnesota, Minneapolis, MN 55455. E-mails: arminzare@umn.edu, mihailo@umn.edu, tryphon@umn.edu.

We focus on turbulent channel flow. The data for our problem originates from high fidelity numerical simulations and consists of partially known velocity correlations [7]–[10]. Our goal is to determine the complete correlation profile of the fluctuating velocity field in a way that is consistent with the underlying dynamics. This is an inverse problem which we formulate as an optimization problem seeking a low-rank representation of the colored-in-time noise component. We use nuclear norm minimization as a surrogate for rank minimization [11]–[16] and provide a customized interior point algorithm which is suitable for solving large-scale problems of this type.

The paper is organized as follows. In Section II, we first explain the stochastically forced linearized NS model. We then relate the linearized system dynamics with the algebraic structure of second-order statistics of channel flow turbulence. In Section III, we formulate the task of completing partially available statistics of the fluctuating velocity field as an optimization problem. To this end, the correlation matrix of all components needs to satisfy a linear equation together with a parameter that characterizes the spectral content of the driving noise. Minimization of the nuclear norm is used as a way to select the low rank noise parameter and to solve this matrix covariance completion problem. In Section IV, we develop a customized algorithm to solve this matrix completion that scales favorably with the size of the problem. In Section V, we apply our techniques to complete flow statistics of a turbulent channel flow. In Section VI, we present concluding thoughts about the scope and potential use of the framework.

II. Background

In this section, we present background material on evolution models for stochastically forced linearized NS equations and second-order statistics of velocity fluctuations.

A. Stochastically forced linearized NS equations

In a turbulent channel flow, with geometry shown in Fig. 1, the dynamics of infinitesimal fluctuations around the mean velocity, $\bar{\mathbf{u}} = [\,U(y)\;\;0\;\;0\,]^T$, are governed by

$$\begin{aligned} \boldsymbol{\psi}_t(y,\boldsymbol{\kappa},t) &= \mathbf{A}(\boldsymbol{\kappa})\,\boldsymbol{\psi}(y,\boldsymbol{\kappa},t) + \mathbf{f}(y,\boldsymbol{\kappa},t), \\ \mathbf{v}(y,\boldsymbol{\kappa},t) &= \mathbf{C}(\boldsymbol{\kappa})\,\boldsymbol{\psi}(y,\boldsymbol{\kappa},t). \end{aligned} \tag{1}$$

Here, $\boldsymbol{\psi} = [\,v_2\;\;\eta\,]^T$ is the state of the linearized model, v_2 and $\eta = \partial_z v_1 - \partial_x v_3$ are the wall-normal velocity and vorticity, $\mathbf{v} = [\,v_1\;\;v_2\;\;v_3\,]^T$ is the fluctuating velocity vector, and $\mathbf{f}$ is a stochastic forcing disturbance. The operator $\mathbf{A}(\boldsymbol{\kappa})$ is the generator of the linearized dynamics, and the

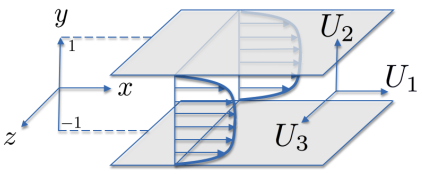

Fig. 1. Geometry of a pressure-driven turbulent channel flow.

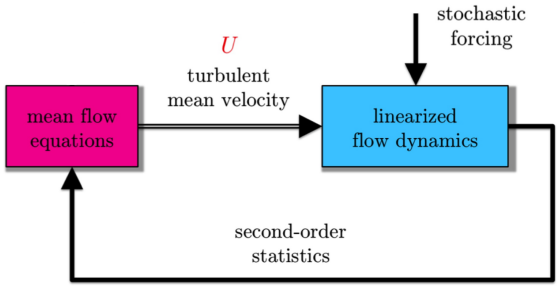

Fig. 2. The statistics of velocity fluctuations are completed by appropriately forcing the linearized dynamics around turbulent mean velocity. Completed second-order statistics can then be brought into the mean flow equations to give turbulent mean velocity and provide equilibrium configuration.

operator $\mathbf{C}(\boldsymbol{\kappa})$ establishes a kinematic relationship between the components of $\boldsymbol{\psi}$ and the components of $\mathbf{v}$,

$$\mathbf{C}(\boldsymbol{\kappa}) \;=\; \begin{bmatrix} \mathbf{C}_{v_1}(\boldsymbol{\kappa}) \\ \mathbf{C}_{v_2}(\boldsymbol{\kappa}) \\ \mathbf{C}_{v_3}(\boldsymbol{\kappa}) \end{bmatrix} \;:=\; \frac{1}{\kappa^2} \begin{bmatrix} \mathrm{i}k_x\,\partial_y & -\mathrm{i}k_z \\ \kappa^2 & 0 \\ \mathrm{i}k_z\,\partial_y & \mathrm{i}k_x \end{bmatrix},$$

where $\boldsymbol{\kappa} = [\,k_x \;\; k_z\,]^T$ denotes the vector of horizontal wavenumbers. A more detailed description of the operators in (1) and the underlying function spaces can be found in [3].

Finite-dimensional approximations $A(\boldsymbol{\kappa})$ and $C(\boldsymbol{\kappa})$ of the operators $\mathbf{A}(\boldsymbol{\kappa})$ and $\mathbf{C}(\boldsymbol{\kappa})$ can be obtained using a pseudospectral scheme with N Chebyshev collocation points in the wall-normal direction [17], thereby resulting into

$$\begin{aligned} \boldsymbol{\psi}_t(\boldsymbol{\kappa},\,t) \;&=\; A(\boldsymbol{\kappa})\,\boldsymbol{\psi}(\boldsymbol{\kappa},\,t) \;+\; \mathbf{f}(\boldsymbol{\kappa},\,t), \\ \mathbf{v}(\boldsymbol{\kappa},\,t) \;&=\; C(\boldsymbol{\kappa})\,\boldsymbol{\psi}(\boldsymbol{\kappa},\,t), \end{aligned} \tag{2}$$

with $\boldsymbol{\psi}(\boldsymbol{\kappa},\,t) \in \mathbb{C}^{2N}$ and $\mathbf{v}(\boldsymbol{\kappa},\,t) \in \mathbb{C}^{3N}$.

B. Second-order statistics of linearized NS equations

At any $\boldsymbol{\kappa}$, the covariance matrix of the velocity vector in (2) is given by,

$$\Phi(\boldsymbol{\kappa}) \;:=\; \lim_{t\,\to\,\infty} \mathcal{E}\left(\mathbf{v}(\boldsymbol{\kappa},\,t)\,\mathbf{v}^*(\boldsymbol{\kappa},\,t)\right),$$

where $\mathcal{E}$ is the expectation operator. This matrix can be obtained from

$$\Phi(\boldsymbol{\kappa}) \;=\; C(\boldsymbol{\kappa})\,X(\boldsymbol{\kappa})\,C^*(\boldsymbol{\kappa}),$$

and it contains all information about the second-order statistics of the fluctuating velocity field in statistical steady-state. Here, X denotes the steady-state covariance matrix of the state in (2)

$$X(\boldsymbol{\kappa}) \;:=\; \lim_{t\,\to\,\infty} \mathcal{E}(\boldsymbol{\psi}(\boldsymbol{\kappa},\,t)\,\boldsymbol{\psi}^*(\boldsymbol{\kappa},\,t)).$$

When system (2) is driven by white-in-time stochastic forcing with second-order statistics,

$$\mathcal{E}\left(\,\mathbf{f}(\boldsymbol{\kappa},\,t_1)\,\mathbf{f}^*(\boldsymbol{\kappa},\,t_2)\,\right) \;=\; M(\boldsymbol{\kappa})\,\delta(t_1 - t_2),$$

the Lyapunov equation

$$A(\boldsymbol{\kappa})\,X(\boldsymbol{\kappa}) \;+\; X(\boldsymbol{\kappa})\,A^*(\boldsymbol{\kappa}) \;=\; -M(\boldsymbol{\kappa}), \tag{3}$$

with $M = M^* \succeq 0$ can be used to find $X(\boldsymbol{\kappa})$.

For a turbulent channel flow, it can be shown that there is no positive semi-definite completion of partially available flow statistics which is consistent with the hypothesis of forcing (2) with white-noise [5], and hence a positive semi-definite M in (3). Thus, the second-order turbulent flow statistics cannot be reproduced by the linearized NS equations with white-in-time stochastic forcing. This limitation can be overcome by departing from white-in-time restriction. In fact, in a more general framework for explaining statistics using linear models, colored-in-time forcing $\mathbf{f}(\boldsymbol{\kappa}, t)$ leads to an indefinite $M(\boldsymbol{\kappa})$ [18]–[20]. Using this framework, a sample covariance $X(\boldsymbol{\kappa}) \succeq 0$, resulting from experiments or high-fidelity numerical simulations, can be made consistent with being covariance of the state in (2). Furthermore, the rank of the matrix $M(\boldsymbol{\kappa})$ provides bounds on the complexity of the spatio-temporal filter that is used to produce colored forcing [6].

III. Completion of Partially Known Statistics

Motivated by the necessity to account for turbulent flow correlations by models of low complexity, we formulate the problem of completing partially available second-order statistics. Data for our problem comes from experiments or high-fidelity numerical simulations. On the other hand, we assume that velocity fluctuations obey the linearized NS equations (1). The statistics of forcing are unknown and sought to explain the given correlations. While the system dynamics impose a linear constraint on the admissible velocity correlations, such an inverse problem admits many solutions for the forcing correlations. We use nuclear norm minimization to obtain correlation structures of low complexity. This complexity translates into dimensionality of spatio-temporal filters that can be used to generate the identified forcing statistics.

The block diagram in Fig. 2 illustrates our modeling procedure. For the linearized dynamics of fluctuations around turbulent mean velocity, the appropriate forcing is sought to reproduce partially available velocity correlations and complete the statistical signature of the turbulent flow field. Completed second-order statistics can then be brought into the mean flow equations in order to give turbulent mean velocity and provide equilibrium configuration.

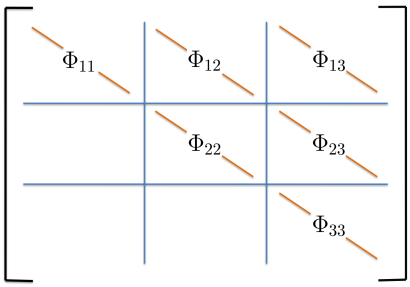

Fig. 3. Publicly available correlations of velocity fluctuations [21] represent diagonal entries of the blocks in the output covariance matrix; cf. (4).

The matrix completion problem can be formulated as,

$$\begin{aligned} \underset{M,\,X}{\text{minimize}} \quad & \|M\|_* \\ \text{subject to} \quad & AX + XA^* + M = 0 \\ & \text{trace}\,(T_k\,X) = g_k, \quad k = 1,\ldots,6N \\ & X \succeq 0. \end{aligned} \tag{MC}$$

Here, matrices A and T_k and scalars g_k denote problem data, Hermitian matrices X and M are optimization variables, and the wavenumber dependence is omitted for notational convenience. In (MC), the nuclear norm, i.e., the sum of singular values of a matrix,

$$\|M\|_* := \sum_{i=1}^{2N} \sigma_i(M),$$

is used as a proxy for rank minimization [11], [14]. The constraint set of (MC) is convex because it is the intersection of three convex sets: the positive semidefinite cone, the linear subspace determined by the Lyapunov constraint, and the linear trace constraints.

The trace constraints in (MC) represent a linear relationship between the steady-state covariance matrix of system (2) and partially available entries of the velocity covariance matrix Φ. Figure 3 illustrates readily available one-point correlations (in the wall-normal direction) resulting from experiments or simulations. The kth diagonal entry of the (i,j)th block of the output covariance matrix, Φ_{ij}, can be computed as,

$$\begin{aligned} & e_k^*\,C_{u_i}\,X\,C_{u_j}^*\,e_k \\ & \quad = \frac{1}{2}\,\text{trace}\left((C_{u_j}^*\,e_k\,e_k^*\,C_{u_i} + C_{u_i}^*\,e_k\,e_k^*\,C_{u_j})\,X\right) \\ & \quad = \text{trace}\,(T_k\,X), \end{aligned} \tag{4}$$

where e_k is the kth unit vector in the standard Euclidean vector space. Here $k = 1,\ldots,N$, where N is the number of collocation points in the wall-normal direction and matrices T_k relate X to the observed statistics from numerical/experimental data. As we show in the next section, such trace constraints are well suited for the purpose of developing customized optimization algorithms.

Since A, T_k, and g_k are parameterized by the horizontal wavenumbers, the solution to (MC) will also be wavenumber-dependent. When dealing with a small number of unknown variables, the convex optimization problem (MC) can be solved using general-purpose solvers [22]. In Section IV, we present an approach that combines a customized interior point algorithm with the alternating direction method of multipliers (ADMM) to solve large problems. ADMM is a method that is well-suited for solving large-scale and distributed optimization problems [23].

IV. Customized algorithm for the matrix completion problem

Interior point methods provide a powerful framework for solving convex optimization problems with inequality constraints [24]. To solve (MC), we develop a customized interior point algorithm that utilizes parameterization of the operator specifying the trace constraints in (MC). As recently shown in [25], this parameterization eliminates the trace constraints and Lyapunov equation from (MC). In each inner iteration of the interior point algorithm, ADMM is used to exploit the respective structures of the log barrier function and the nuclear norm. The computational steps involve application of the BFGS algorithm and a convenient singular value thresholding.

A. Null space parameterization

Trace constraints in (MC) define a linear mapping

$$\mathcal{T}\,(X) = \mathbf{g}, \tag{5}$$

from the hermitian matrix X to the vector $\mathbf{g} := \text{col}\,\{g_k\}$. Thus, all solutions to (5) can be parameterized using the null space of the linear operator $\mathcal{T}$,

$$X = X_0 + \sum_{j=1}^{q} x_j\,X_j. \tag{6}$$

Here, q denotes the size of the null space of the operator $\mathcal{T}$, X_0 is a particular solution to (5), x_j's are real parameters, and the matrices X_j are linearly independent solutions of

$$\text{trace}\,(T_k\,X_j) = 0, \quad k = 1,\ldots,6N, \quad j = 1,\ldots,q. \tag{7}$$

For the purpose of solving the matrix completion problem we will constrain our choice of a particular solution to (5) to the positive-semidefinite cone. To obtain $X \succeq 0$, we solve the following optimization problem

$$\begin{aligned} \underset{X_0}{\text{minimize}} \quad & -\log\det\,(X_0) \\ \text{subject to} \quad & \text{trace}\,(T_k\,X_0) = g_k, \quad k = 1,\ldots,6N \end{aligned} \tag{8}$$

where the positive-definiteness of X_0 is implicitly enforced via the $\log\det$ objective function. The convexity of this optimization problem follows from convexity of the objective function and linearity of the trace constraints [24]. While general purpose SDP solvers can efficiently handle problems of small and medium size, we have developed an efficient quasi-Newton algorithm for large problems. Due to page limitation details of our algorithm will be reported elsewhere.

To complete the parameterization we must find basis matrices, X_j, that span the null space of $\mathcal{T}$. Since matrices T_k in (7) can be separated into real and imaginary parts,

$$T_k \;=\; \mathrm{Re}\,(T_k) \;+\; \mathrm{i}\,\mathrm{Im}\,(T_k),$$

the null space of the linear operator $\mathcal{T}$ can also be decomposed into two linearly independent parts. Thus, we can compute the null space of the real and imaginary parts separately and concatenate the resulting basis elements. This allows us to work with real valued matrices which is advantageous when dealing with large null spaces. The null space of $\mathcal{T}$ is computed via the singular value decomposition of a matrix T, whose columns are obtained by vectorizing matrices T_k,

$$T \;=\; \left[\; \mathrm{vec}(T_1) \;\vdots\; \mathrm{vec}(T_2) \;\vdots\; \cdots \;\vdots\; \mathrm{vec}(T_{6N}) \;\right]_{4N^2\times 6N}.$$

The singular value decomposition of the fat matrix T^T

$$T^T \;=\; U\,\Sigma\,V^T,$$

is used to obtain

$$\mathcal{N}ull\,(T^T) \;=\; \{v_{r+1}, v_{r+2}, \ldots, v_{4N^2}\},$$

where r is the number of nonzero singular values of T^T and v_i is the ith column of V. By de-vectorizing the null space of T^T we obtain the matrices that form the null space of the operator $\mathcal{T}$. This completes the parameterization of X in (6).

A similar parameterization can be considered for M by substituting (6) into the Lyapunov equation,

$$M \;=\; -\,(\,A\,X \;+\; X\,A^*\,) \;=\; M_0 \;+\; \sum_{j=1}^{q} x_j\,M_j,$$

where

$$M_0 \;=\; -\,(A\,X_0 \;+\; X_0\,A^*), \quad M_j \;=\; -\,(A\,X_j \;+\; X_j\,A^*).$$

This procedure eliminates the equality constraints from (MC) but adds real parameters, x_j, to the set of optimization variables.

B. Interior point algorithm

The discussion in the previous section allows us to parameterize solutions for X and M by introducing a new optimization variable $x = \begin{bmatrix} x_1 & x_2 & \ldots & x_q \end{bmatrix}^T$. Based on this, problem (MC) can be reformulated as

$$\begin{array}{ll} \underset{x,\,M}{\text{minimize}} & \|M\|_* \;-\; \dfrac{1}{\tau}\,\log\det\,(X_0 + \displaystyle\sum_{j\,=\,1}^{q} x_j\,X_j) \\ \text{subject to} & \displaystyle\sum_{j=1}^{q} x_j\,M_j \;-\; M \;+\; M_0 \;=\; 0. \end{array} \tag{9}$$

Convexity of the objective function in conjunction with linearity of the constraint implies convexity. The logarithmic barrier function in (9) guarantees positive definiteness of the state covariance matrix X. On the other hand, parameter τ determines the relative importance of the objective and barrier functions. The outer steps of the interior point algorithm results in the convergence to the optimal solution as $\tau \to \infty$ and it is summarized next:

given: strictly feasible M, x, tolerance $\epsilon > 0$

repeat:

1. compute M^* and x^* (solutions to (9))
2. $M \Leftarrow M^*$ and $x \Leftarrow x^*$
3. if $1/\tau \leq \epsilon$, return(M, x)
4. increase τ; $\tau^+ = \mu\tau \quad (\mu \approx 10 \sim 100)$.

Step 1 involves the inner iterations in which first or second-order optimization methods can be used to find the optimal solution to (9) for a specific τ. Outer iterations generate a sequence of points on the central path to optimality [24].

The log-det barrier in (9) was introduced to guarantee positive definiteness of the state covariance matrix. Our attempts to enforce positive definite constraints in (MC) via projections to the positive semi-definite cone [26], [27] have not been successful. While we suspect that this is because of ill-conditioning of the dynamical generator in the Lyapunov-like constraint, this issue requires additional scrutiny and it will be examined in our future research.

C. Alternating direction method of multipliers

For a fixed value of τ, we use ADMM to solve (9). The augmented Lagrangian associated with (9) is given by

$$\begin{aligned} \mathcal{L}_\rho(x, M, \Lambda) \;=\; & \|M\|_* \;-\; \frac{1}{\tau}\,\log\det\,(X_0 + \sum_{j=1}^{q} x_j X_j) \\ & +\; \mathrm{trace}\,(\Lambda^*(\sum_{j=1}^{q} x_j\,M_j - M + M_0)) \\ & +\; \frac{\rho}{2}\,\|\sum_{j=1}^{q} x_j\,M_j - M + M_0\|_F^2, \end{aligned}$$

where Λ is the Lagrange multiplier, ρ is a positive scalar, and $\|\cdot\|_F$ is the Frobenius norm.

The ADMM algorithm uses a sequence of iterations to find the minimizer of the constrained optimization problem (9),

$$x^{k+1} \;:=\; \underset{x}{\arg\min}\; \mathcal{L}_\rho\,(x,\,M^k,\,\Lambda^k) \tag{10a}$$

$$M^{k+1} \;:=\; \underset{M}{\arg\min}\; \mathcal{L}_\rho\,(x^{k+1},\,M,\,\Lambda^k) \tag{10b}$$

$$\Lambda^{k+1} \;:=\; \Lambda^k \;+\; \rho\,(\sum_{j=1}^{q} x_j^{k+1} M_j - M^{k+1} + M_0) \tag{10c}$$

and is terminated when the convergence tolerances are met,

$$\begin{aligned} \|\sum_{j=1}^{q} x_j^{k+1} M_j - M^{k+1} + M_0\|_F \;&\leq\; \epsilon_1, \\ \|M^{k+1} - M^k\|_F \;&\leq\; \epsilon_2, \\ \|x^{k+1} - x^k\|_2 \;&\leq\; \epsilon_3. \end{aligned}$$

The Appendix provides solutions to (10a) and (10b).

Upon convergence of the ADMM algorithm, one outer iteration of the interior point algorithm has been completed. Successive iterations, where τ is increased to force the objective towards the low rank solution, follow a similar computational routine.

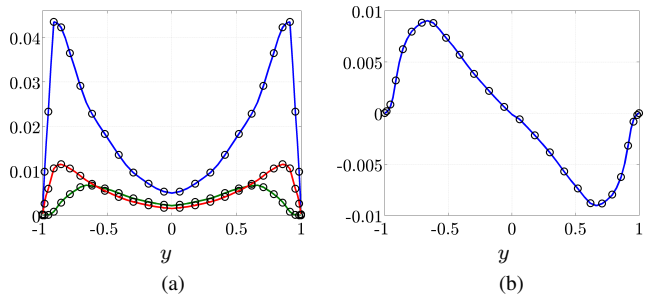

Fig. 4. Correlation profiles at $\boldsymbol{\kappa} = (k_x, k_z) = (2.5, 7)$ for a turbulent channel flow with $R_\tau = 186$. Perfect agreement between velocity correlations resulting from numerical simulations [7], [8] (–) and the solution to (MC) is observed for both (a) normal (blue: $\mathrm{diag}\,(\Phi_{11})$, green: $\mathrm{diag}\,(\Phi_{22})$, red: $\mathrm{diag}\,(\Phi_{33})$) and (b) shear stress ($-\mathrm{diag}\,(\Phi_{12})$) profiles.

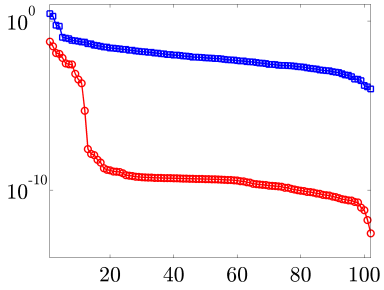

Fig. 5. Singular values of the low-rank solution M resulting from (MC) ($\circ$) and from the feasibility problem ($\square$) for $\boldsymbol{\kappa} = (k_x, k_z) = (2.5, 7)$.

V. Application to a Turbulent Channel Flow

In this section we apply our techniques to complete partially available statistics of a turbulent channel flow with $R_\tau = 186$. These publicly available statistics [21] come from numerical simulations of the nonlinear NS equations [7], [8]. As illustrated in Fig. 3, they contain one-point velocity correlations (in the wall-normal direction) at various horizontal wavenumbers. Using the completion problem (MC), we identify noise models of low-complexity that reproduce the statistical signatures of turbulent velocity fluctuations.

The differential operators are discretized using $N = 51$ collocation points in y. In the horizontal directions, 50×51 wavenumbers are used, $k_x \in [0.01,\, 42.5]$ and $k_z \in [0.01,\, 84.5]$, with the largest values of k_x and k_z being equal to those used in numerical simulations that generated our data [7], [8].

The energy spectrum of velocity fluctuations is given by

$$E(\boldsymbol{\kappa}) \;=\; (1/2)\,\mathrm{trace}\,(\Phi(\boldsymbol{\kappa}))\,.$$

The peak of the premultiplied energy spectrum occurs at $(k_x,\, k_z) \approx (2.5, 7)$. Figure 4 illustrates that all one-point velocity correlations at this wavenumber pair are reproduced by the identified colored-in-time forcing. It should be noted that the problem (MC) is not feasible for $M \succeq 0$. This implies that perfect matching of turbulent flow statistics could not have been accomplished under whiteness-in-time restriction.

We next examine the singular values of the matrix M that results from the matrix completion problem (MC). As shown in Fig. 5, at $(k_x,\, k_z) \approx (2.5, 7)$, M has 11 dominant singular values. On the other hand, there is no clear-cut in the singular values of M which comes from the feasibility problem (8). The approximately low-rank matrix M has 7 significant positive eigenvalues (0.0323, 0.0115, 0.0068, 0.0031, 0.0027, 0.0008, 0.0002) and 4 significant negative eigenvalues (-0.0610, -0.0129, -0.0028, -0.0004). Based on the developments of [6], 7 colored-in-time inputs are needed to account for the given partial state statistics in (MC).

To demonstrate the performance of our approach at other wavenumbers we compute the one-dimensional energy spectra of velocity correlations and compare them with data resulting from direct numerical simulations. Figure 6 shows the pre-multiplied one-dimensional energy spectra of streamwise velocity fluctuations as a function of streamwise or spanwise wavelengths, $\lambda_x^+ := R_\tau(2\pi/k_x)$ and $\lambda_z^+ := R_\tau(2\pi/k_z)$, and the wall-normal coordinate, $y^+ := R_\tau(1+y)$, all in inner (viscous) units. Color plots and contour lines respectively represent the pre-multiplied energy spectra resulting from numerical simulations [7], [8] and our optimization framework. These are in perfect agreement. Similar results are obtained in reproducing one-dimensional energy spectra of the wall-normal and spanwise velocity fluctuations, as well as shear stress ($\mathrm{diag}\,(\Phi_{12})$).

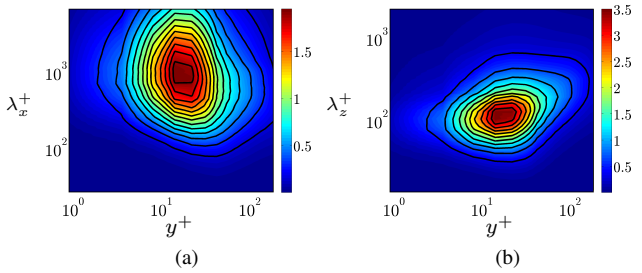

Fig. 6. Pre-multiplied, one-dimensional energy spectra of streamwise velocity fluctuations; (a) $k_x \mathrm{diag}\,(\Phi_{11})\,(k_x, y^+)$, (b) $k_z \mathrm{diag}\,(\Phi_{11})\,(k_z, y^+)$. Color plots: spectra resulting from numerical simulations [7], [8]. Contour lines: spectra resulting from the solution to (MC).

VI. Concluding Remarks

We have examined the problem of completing partially available statistics of turbulent flows using stochastically forced linearized NS equations. In contrast to previous studies, a colored-in-time forcing model was assumed to drive the linearized dynamics. To complete the statistical signature of the turbulent velocity field with low-complexity colored-in-time forcing, we formulate a new class of structured matrix completion problems. For this purpose, minimization of the nuclear norm was used as a way to select the low rank noise parameter and to complete data which is not available. To solve this problem, we utilize null space parameterization techniques along with a customized interior point algorithm.

ACKNOWLEDGMENTS

The authors would like to thank Dr. Fu Lin for useful discussions.

APPENDIX

A. Solution to the x-minimization problem (10a)

For fixed $\{x^k,\, M^k,\, \Lambda^k\}$, the augmented Lagrangian $\mathcal{L}_\rho$ is minimized with respect to the vector x,

$$\begin{aligned}\underset{x}{\text{minimize}} \quad & -\frac{1}{\tau}\,\log\det\,(X_0+\sum_{j=1}^{q} x_j X_j) \\ & +\frac{\rho}{2}\,\|\sum_{j=1}^{q} x_j M_j \;-\; U^k\|_F^2\end{aligned}$$

where $U^k := M^k - M_0 - (1/\rho)\Lambda^k$. The gradient and Hessian of this objective are given by

$$\begin{aligned}\frac{\partial \mathcal{L}_\rho}{\partial x_i} \;&=\; -\frac{1}{\tau}\,\mathrm{trace}\,(\,Y\,X_i\,) \\ &\quad +\rho\,\mathrm{trace}\,(\,(\sum_{l=1}^{q} x_l X_l)\,M_i - U^k\,M_i\,), \\ \frac{\partial^2 \mathcal{L}_\rho}{\partial x_i \partial x_j} \;&=\; \frac{1}{\tau}\,\mathrm{trace}\,(\,Y\,X_i\,Y\,X_j\,) \;+\; \rho\,\mathrm{trace}\,(M_i\,M_j),\end{aligned}$$

where $Y \;:=\; (\,X_0 \;+\; \sum_{l=1}^{q} x_l X_l\,)^{-1}$. Newton or quasi-Newton (e.g. BFGS) methods can be used to solve this sub problem efficiently.

B. Solution to the M-minimization problem (10b)

For fixed $\{x^{k+1},\, M^k,\, \Lambda^k\}$, the augmented Lagrangian is minimized with respect to M,

$$\underset{M}{\text{minimize}} \quad \|M\|_* \;+\; \frac{\rho}{2}\|M - V^k\|_F^2 \tag{12}$$

where $V^k := (1/\rho)\Lambda^k + M_0 + \sum_{l=1}^{q} x_l^k M_l$. The solution to (12) is qiven by the singular value thresholding operator [28]. For this purpose we must first compute the singular value decomposition of the symmetric matrix

$$V^k \;=\; U\,\Sigma\,U^*,$$

and apply the soft-thresholding operator to it's singular values

$$\mathcal{S}_{1/\rho}(\Sigma) \;=\; \mathrm{diag}\,(\sigma_i - 1/\rho)_+\,,$$

where $a_+ = \max\{a, 0\}$. The solution to the M-minimization problem will thus be determined by

$$M^{k+1} \;=\; U\,\mathcal{S}_{1/\rho}(\Sigma)\,U^*.$$

REFERENCES

[1] B. F. Farrell and P. J. Ioannou, "Stochastic forcing of the linearized Navier-Stokes equations," *Phys. Fluids A*, vol. 5, no. 11, pp. 2600–2609, 1993.

[2] B. Bamieh and M. Dahleh, "Energy amplification in channel flows with stochastic excitation," *Phys. Fluids*, vol. 13, no. 11, pp. 3258–3269, 2001.

[3] M. R. Jovanović and B. Bamieh, "Componentwise energy amplification in channel flows," *J. Fluid Mech.*, vol. 534, pp. 145–183, July 2005.

[4] R. Moarref and M. R. Jovanović, "Model-based design of transverse wall oscillations for turbulent drag reduction," *J. Fluid Mech.*, vol. 707, pp. 205–240, September 2012.

[5] M. R. Jovanović and T. T. Georgiou, "Reproducing second order statistics of turbulent flows using linearized Navier-Stokes equations with forcing," in *Bulletin of the American Physical Society*, Long Beach, CA, November 2010.

[6] Y. Chen, M. R. Jovanović, and T. T. Georgiou, "State covariances and the matrix completion problem," in *Proceedings of the 52nd IEEE Conference on Decision and Control*, Florence, Italy, 2013, pp. 1702–1707.

[7] J. C. Del Alamo and J. Jimenez, "Spectra of the very large anisotropic scales in turbulent channels," *Physics of Fluids*, vol. 15, no. 6, pp. 41–44, 2003.

[8] J. C. Del Alamo, J. Jimenez, P. Zandonade, and R. D. Moser, "Scaling of the energy spectra of turbulent channels," *Journal of Fluid Mechanics*, vol. 500, pp. 135–144, 2004.

[9] J. Jimenez, J. C. Del Alamo, and O. Flores, "The large-scale dynamics of near-wall turbulence," *Journal of Fluid Mechanics*, vol. 505, pp. 179–199, 2004.

[10] S. Hoyas and J. Jimenez, "Scaling of the velocity fluctuations in turbulent channels up to $Re_\tau = 2003$," *Physics of Fluids*, vol. 18, no. 1, p. 011702, 2006.

[11] M. Fazel, "Matrix rank minimization with applications," Ph.D. dissertation, PhD thesis, Stanford University, 2002.

[12] E. J. Candès and B. Recht, "Exact matrix completion via convex optimization," *Foundations of Computational mathematics*, vol. 9, no. 6, pp. 717–772, 2009.

[13] R. H. Keshavan, A. Montanari, and S. Oh, "Matrix completion from a few entries," *Information Theory, IEEE Transactions on*, vol. 56, no. 6, pp. 2980–2998, 2010.

[14] B. Recht, M. Fazel, and P. A. Parrilo, "Guaranteed minimum-rank solutions of linear matrix equations via nuclear norm minimization," *SIAM review*, vol. 52, no. 3, pp. 471–501, 2010.

[15] E. J. Candes and Y. Plan, "Matrix completion with noise," *Proceedings of the IEEE*, vol. 98, no. 6, pp. 925–936, 2010.

[16] R. Salakhutdinov and N. Srebro, "Collaborative filtering in a non-uniform world: Learning with the weighted trace norm," *Advances in Neural Information Processing Systems 24*, 2011.

[17] J. A. C. Weideman and S. C. Reddy, "A MATLAB differentiation matrix suite," *ACM Transactions on Mathematical Software*, vol. 26, no. 4, pp. 465–519, December 2000.

[18] T. T. Georgiou, "Spectral estimation via selective harmonic amplification," *Automatic Control, IEEE Transactions on*, vol. 46, no. 1, pp. 29–42, 2001.

[19] T. T. Georgiou, "The structure of state covariances and its relation to the power spectrum of the input," *IEEE Trans. Autom. Control*, vol. 47, no. 7, pp. 1056–1066, 2002.

[20] T. T. Georgiou, "Spectral analysis based on the state covariance: the maximum entropy spectrum and linear fractional parametrization," *IEEE Trans. Autom. Control*, vol. 47, no. 11, pp. 1811–1823, 2002.

[21] [Online]. Available: http://torroja.dmt.upm.es/channels/data/

[22] M. Grant and S. Boyd, "CVX: Matlab software for disciplined convex programming, version 1.22," Sept. 2012.

[23] S. Boyd, N. Parikh, E. Chu, B. Peleato, and J. Eckstein, "Distributed optimization and statistical learning via the alternating direction method of multipliers," *Foundations and Trends in Machine Learning*, vol. 3, no. 1, pp. 1–122, 2011.

[24] S. Boyd and L. Vandenberghe, *Convex optimization*. New York: Cambridge University Press, 2004.

[25] F. Lin, M. R. Jovanović, and T. T. Georgiou, "An ADMM algorithm for matrix completion of partially known state covariances," in *Proceedings of the 52nd IEEE Conference on Decision and Control*, Florence, Italy, 2013, pp. 1684–1689.

[26] M. Fazel, T. K. Pong, D. Sun, and P. Tseng, "Hankel matrix rank minimization with applications to system identification and realization," *SIAM Journal on Matrix Analysis and Applications*, vol. 34, no. 3, pp. 946–977, 2013.

[27] Z. Wen, D. Goldfarb, and W. Yin, "Alternating direction augmented lagrangian methods for semidefinite programming," *Mathematical Programming Computation*, vol. 2, no. 3-4, pp. 203–230, 2010.

[28] J.-F. Cai, E. J. Candès, and Z. Shen, "A singular value thresholding algorithm for matrix completion," *SIAM Journal on Optimization*, vol. 20, no. 4, pp. 1956–1982, 2010.